Model Evaluation of Soil Factors Affecting Rigid Pavement Pumping

WAIN W. STOWE, U. S. Army Corps of Engineers;
RICHARD L. HANDY, Iowa State University; and
JAMES P. FERO, U. S. Army Corps of Engineers

A laboratory model was devised to simulate pumping of an 8-in. nonreinforced rigid pavement under a 9,000-lb wheel load traveling 14 mph. The model pumping action was observed to be a soil erosion phenomenon, and a theoretical approach indicated soil cohesion as a key factor. Tests on several fine-grained soils at different temperatures and different compacted densities verified that pumping rate without drainage is inversely proportional to soil cohesion. Increasing soil density and decreasing soil temperature both retard pumping by increasing cohesion, and stabilizers to inhibit pumping of fine-grained soils may be selected on the basis of their effect on cohesion. Preliminary pumping data on soil-cement are presented.

•PUMPING has been recognized as a major cause of concrete pavement failure since 1945. Although regarded in many states as a minor problem (1, p. 163), pumping was a causal factor in the majority of AASHO Road Test rigid pavement failures (2), and may be expected to increase with increasing truck traffic.

Pumping may be defined as the ejection of soil and water from beneath a rigid pavement, induced by the deflection of the slab at a joint, edge, or crack (Fig. 1a). Heavy axle loads are normally required to deflect the slab sufficiently to promote pumping. Since free water is also required, pumping normally occurs only during or immediately following a rain. The ejection of soil and water forms a void which continues to enlarge until the slab cracks and fails.

During the 1940's exhaustive field surveys were conducted to find the causes of pumping. Results of surveys in Tennessee, North Carolina, Kansas, Illinois, and Indiana (3) concluded that: (a) slow, heavily loaded trucks induce the most pumping; (b) pumping is most severe on uphill grades where truck speed is lowered; (c) pumping soils have over 45 percent combined silt and clay; (d) there is no correlation of pumpability to consolidation and shear strength, although compaction delays pumping; and (e) a granular subbase will prevent pumping.

Since the 1950's many highways have been built on granular subbases, which solved the problem at least temporarily. However, under increasingly severe loading conditions even granular subbases were found to pump or blow, the latter being defined as ejection of granular base materials in an action similar to pumping (1), but usually occurring along slab edges rather than at joints (Fig. 1b). For the present purpose we make no distinction between pumping and blowing, and soil includes granular or treated base or subbase materials immediately beneath the pavement slab.

Paper sponsored by Committee on Strength and Deformation Characteristics of Pavement Sections.

Figure 1. (a) Pavement pumping; ejection of mud and water; (b) blowing; ejection of sand and water.

LABORATORY MODELS

A model approach allows isolation and evaluation of pertinent variables at the expense of introducing uncertainties regarding the relationship between the model and the field prototype situation. In 1957 a model was built by the Portland Cement Association (4) to about one-half scale; it had a 2-in. thick concrete slab, and required 2 cu yd of base material. The slabs were loaded simultaneously, an action not occurring under actual pavements.

Principal findings from the PCA study were that better compaction reduces granular subbase pumping. Pumping was observed in subbase material containing more than 10 percent passing the No. 200 sieve. Use of a subbase reduced pumping, and a granular soil-cement did not pump.

Another model was devised about the same time by Havers and Yoder (5), using an 8- by 6-in. vertically oriented cylindrical sample agitated by a piston from above. The pumping action was recognized as involving not only an erosion by the ejection of water, but also a migration and selective removal of fines from a base course, and an upward intrusion of subgrade material into a base course. Again, the loading did not duplicate the one-two slap action of slabs at pavement joints. Their results indicated that (a) a highly plastic residual clay from weathering of limestone (Frederick series) pumped less than a moderately plastic silty clay glacial soil (Crosby series); (b) increased compaction decreased deflections; (c) increased pavement pressure increased pumping; and (d) an open-graded base pumps less than one containing generous amounts of fines. A further study by Chamberlin and Yoder (6) indicated that the critical contents of minus 200 sieve material to cause pumping are over 3 percent for a gravel base or over 12 percent for a sand base.

These model studies of pumping emphasized gradation effects, and filter design theory was suggested to prevent selective grain movements or intrusions.

A smaller model was designed by Reign in 1961 (7). He utilized a 2- by 2-in. cylindrical soil sample with the load applied in a sinusoidal fashion from two semicircular plates which remained in contact with the soil. Reign found a correlation to group index; the higher the index over 4, the more the pumping. Although the model represented the alternating loading condition at a joint, it did not simulate the sudden slap received by the soil under the departure slab as the load crosses the joint. Also, the edge effects from the small sample and calibration problems made correlation of data difficult.

Another model, devised by the authors in 1963, is used in this study. The objectives were to devise a realistic model and attempt to evaluate the effects of various factors such as temperature, soil type, density, texture, shearing strength, and effects of stabilizers.

DESCRIPTION OF APPARATUS

The essential elements of the model are shown in Figure 2a. A 31-in. diameter drive wheel with eight 3-in. diameter rubber rollers to transmit the load is mounted

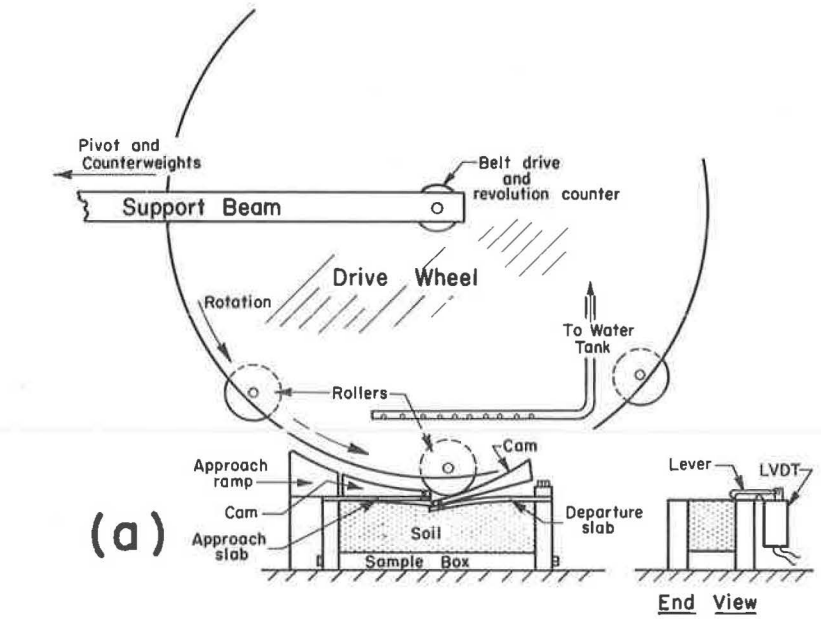

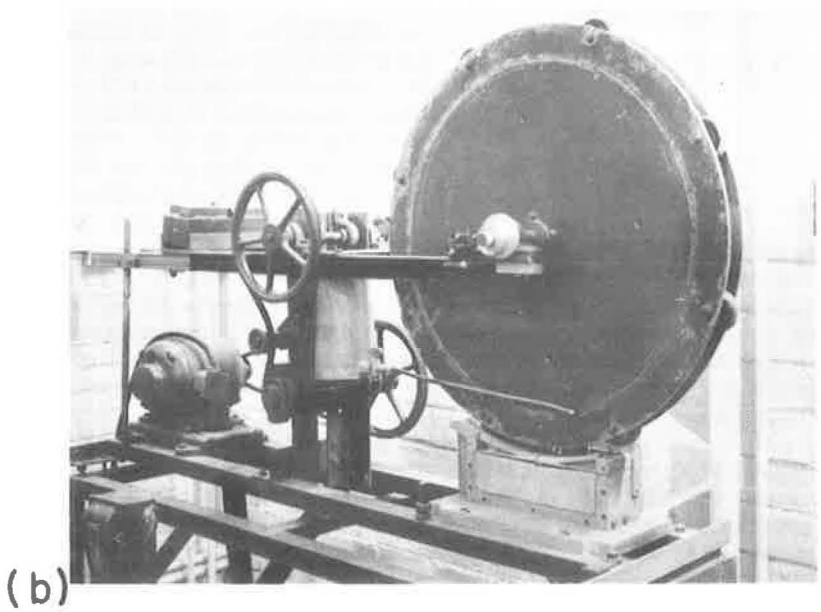

Figure 2. (a) Schematic of pumping apparatus. Soil sample is 3 by 3 by 11 ¼ in.; rollers are 3-in. diameter and move at 3 mph. (b) Overall view of the pumping apparatus with plexiglass sample box front removed to show soil-cement sample after pumping.

at the end of a 5-ft beam, 2 ft from a pivot. An adjustable weight is attached to the beam beyond the pivot as a counterbalance, and an electric motor turns the drive wheel at an angular velocity of 30 rpm. A sample box to hold standard 3- by 3- by 11 ¼-in. compacted flexural test specimens (ASTM Designation D 1632-63 (8)) is cen-

tered under the axis of the drive wheel. The simulated pavement slabs are $\frac{1}{16}$-ft sheet titanium, chosen for its high resistance to fatigue.

One problem was to translate the arc path of the rollers to the horizontal plane of the slabs; this was done with aluminum cams concave to the path of the rollers (16 $\frac{1}{2}$-in. radius) and attached near the slab joint to allow uniform bending of the slabs as the load crosses.

A second problem was how to avoid impact loading of the approach slab. This was done with an aluminum ramp bolted to the sample box; as one roller leaves the departure slab, the weight of the drive wheel is transferred to the next roller on this approach ramp.

Deflections are measured at two locations on each slab, at the middles and at the joints. Vertical displacements of the slabs are transmitted by levers (Fig. 2a) to cores inside four linear variable differential transformers (LVDT's). The LVDT's convert the linear deflections into discrete a.c. voltage changes which are sent to rectifiers, amplifiers, and a four-channel rapid scan recorder. A microswitch on the large wheel actuates an event counter on the recorder every eight repetitions of loading. Thus the amounts of deflection vs number of repetitions are continuously plotted on the recorder chart.

MODEL ANALYSIS

The machine was originally conceived to be analogous to an 18,000-lb axle load traveling at various speeds. A preliminary analysis was performed by considering relative tire print sizes and their contact times. Prints from the model tires average 0.375 sq in., so for a contact pressure of 75 psi the roller load must be 28 lb. As a check, the load giving a maximum slab contact pressure of 7 psi, to correspond to the PCA experiments (3), was calculated, taking 100 pci as the modulus of subgrade reaction. Calculated this way, the model tire load is 26.5 lb.

The model tire print length is 0.50 in., compared to about 10 in. measured on a loaded truck, which means that for the same tire contact time at any point as a truck traveling at 60 mph, the model wheel should travel 3 mph.

The 28 lb and 3 mph were used for design. A more sophisticated model analysis revealed some inconsistencies and velocity distortions, a distorted model being inevitable because it is impossible to scale down all the various soil and fluid factors.

A partial list of variables might include:

n^*, number of repetitions;
W, wheel load, M;
V, wheel velocity, LT^{-1};
A, wheel contact area, L^2;
L, acting slab length, L;
P, acting slab perimeter, L;
d^*, deflection, L;
s^*, any soil grain size, L;
ρ^*, density of fluid, ML^{-3};
μ^* viscosity of fluid, $ML^{-1}T^{-1}$;
σ^*, surface tension of fluid, MT^{-2};
E, slab modulus of elasticity, ML^{-2};
I, slab moment of inertia, L^{-2}; and
g^*, acceleration of gravity, LT^{-2}.

Variables not scaled in the model are starred. (Others whould include soil specific gravity, cohesion, density, and moisture content.) From these variables, a series of dimensionless π terms may be written:

$$n = f\left(\frac{d}{s}, \frac{W}{A\rho s}, \frac{V^2}{gP}, \frac{\rho V^2 P}{\sigma}, \frac{\rho V P}{\mu}, \frac{L}{P}, \frac{L^2}{A}, \frac{L}{s}, \frac{WL^2}{EI}, \frac{AE}{W}\right) \quad (1)$$

According to principles of similitude, corresponding π terms should be equal in the model and in the prototype field situation (9). If this is true or if the distortions are

of no consequence, n, the number of repetitions, should be equivalent in model and prototype.

The condition of equality of the second π term is readily satisfied, i.e., since s is the same in the model as in the prototype, d should be the same also; if a deflection of 0.10 in. is taken as incipient failure in the pavement, 0.10 in. is the analogous deflection in the model. The third term dictates that W/A should be the same in model and prototype; both are nominally 75 psi. The fourth, fifth, and sixth terms cannot be simultaneously satisfied. They are dimensionally analogous to the Froude, Weber and Reynolds numbers, representing inertial, surface tension, and viscous effects, respectively. For reasons discussed later relating erosion to impulse and momentum, the Froude number appears most pertinent, and the other two terms were ignored. According to the fourth π term, if the field pumping perimeter P is 25 ft, the truck speed corresponding to a model speed Vm of 3 mph is only about 14 mph. The velocity variable was to have been investigated, but could not be because of lack of affluent sponsors. As previously mentioned, field data indicate more pumping at low than at high vehicular speeds (3).

The seventh π term, L/P, for the model is 0.394, so for a field active or pumping perimeter of 25 ft, the length of cantilever slab L should be about 10 ft. In the absence of actual measurements all that can be said is that this appears to be the correct order of magnitude. The analogous dimension for edge pumping would be some diagonal vector representing the direction of water movement, about which even less is known. The eighth term suggests a constant ratio between L and tire print length; scale factors for both are about 20. The ninth term, L/s, is necessarily distorted and we assume it is not important. The tenth term which describes bending in flexure is approximately satisfied, the $\frac{1}{16}$-in. titanium model slab corresponding to about 8 in. of nonreinforced concrete. The last term is indicative of slab warping under the respective wheel loads and indicates warping will be less in the model.

To summarize, the pumping machine is a distorted model with horizontal linear dimension scale factors of about 20, and vertical deflection, soil and fluid property, and unit load scale factors of one. Contrary to original plan, the model was only operated at one speed, corresponding to a truck speed of about 14 mph.

EROSION

Model trials indicated that pumping is essentially an erosion phenomenon, material under the model slabs being eroded and removed with the ejecting water. Erodibility of sediments at various water velocities was plotted by Hjulstrom (10), who found that fine sands are most readily eroded, both coarser and finer sizes being more resistant. Resistance of clay was attributed to cohesion.

An influence from clay mineralogy is suggested by a soil erosion study by Lutz (11), who found that calcium saturation decreased erodibility of a montmorillonitic soil (Iredell series), and that a kaolinitic clay soil (Davidson series) was even less erodible. Lutz' results may have been strongly influenced by permeability and infiltration rates. Erosion by artificial raindrops also increases with increasing sand and decreases with aggregation (12, p. 38). André and Anderson suggest that erodibility depends on the ratio of binder (clay) to readily erodible particles (sand) (13).

Horton (14) applied principles of fluid mechanics to the open flow erosion process, theorizing that erosion will take place when the force provided by the flow of water exceeds the shearing resistance of the soil. Horton's equation, derived on the basis of energy considerations, relates erosive force to slope and depth of flow.

Another approach is a fluid mechanics consideration of impulse and momentum, which shows that drag on a body by a fluid of density ρ and constant velocity, V_f, relative to the body is

$$D = k_D \rho a_y V_f^2 \qquad (2)$$

where

D = drag,

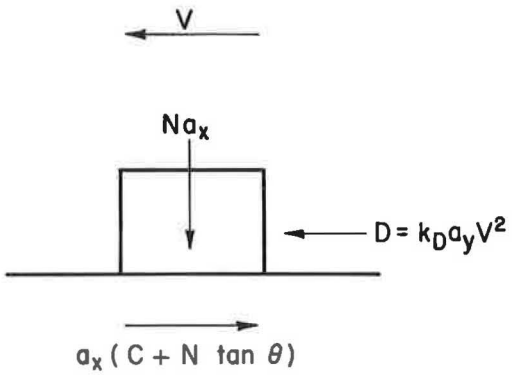

Figure 3. Erosive and resistant forces on a soil grain.

k_D = a drag coefficient, and

a_y = the area of the object normal to the direction of flow.

Opposing D is shear (Fig. 3), or for incipient erosion,

$$D \geq a_x g(c + N \tan \theta) \qquad (3)$$

where

a_x = grain base contact area,
g = acceleration of gravity,
c = unit cohesive shear strength of contact,
N = normal stress from immersed weight of soil grain, and
tan θ = coefficient of sliding friction at contact[a].

For a cubic grain,

$$a_x = d^2, \text{ and} \qquad (4)$$

$$N = d(\rho_s - \rho) \qquad (5)$$

where ρ_s is the density of the grain. Substituting and combining equations,

$$D = k_d \rho \; V_f^2 \; d^2 \geq g d^2 \left[c + d(\rho_s - \rho) \tan \theta \right] \qquad (6)$$

$$V_f^2 \geq \frac{g}{k_d \rho} \left[c + d(\rho_s - \rho) \tan \theta \right]$$

or

$$V_f^2 \geq C \left[c + d(\rho_s - \rho) \tan \theta \right] \qquad (7)$$

where C may be called a coefficient of erosion, and will vary somewhat depending on grain shape and alignment. (Dimensions of C are $L^4 T^{-2} M^{-1}$)[b].

Therefore, if unit cohesion c = 0, as for sand or gravel, the erosion velocity, V, should be proportional to the square root of the grain diameter.

Or if the grain size, d, or the coefficient of friction are very small, as for a clay, erosion velocity, V, should be proportional to square root of the cohesion (more correctly the cohesive shear strength).

The relationship between V and erosion rate will be through some unknown probability function. That is, fluid velocities in turbulent flow have an exceedingly random distribution about an average; raising V, the threshold for erosion, should reduce the probability of encountering a fluid velocity sufficient to erode, and hence reduce the rate of erosion.

---

[a] Tan θ was used rather than tan φ to distinguish sliding friction from internal friction, which is influenced by bulking during shear.

[b] A similar approach by Leopold, Wolman and Miller (12, p. 172) assumes that the force to move the particle must overcome the weight of the particle; presumably the initial movement would be by tipping rather than sliding, as assumed previously. Making no allowance for cohesion, they also concluded that V for erosion is proportional to $\sqrt{d}$, and point out that in open channel flow $V_f \simeq \sqrt{\tau}$, where τ is the resistance to flow, and therefore $d \simeq \tau$. This they illustrate with experimental data. In another derivation after Leopold (12, p. 175) frictional resistance is considered, but again cohesion is not taken into account.

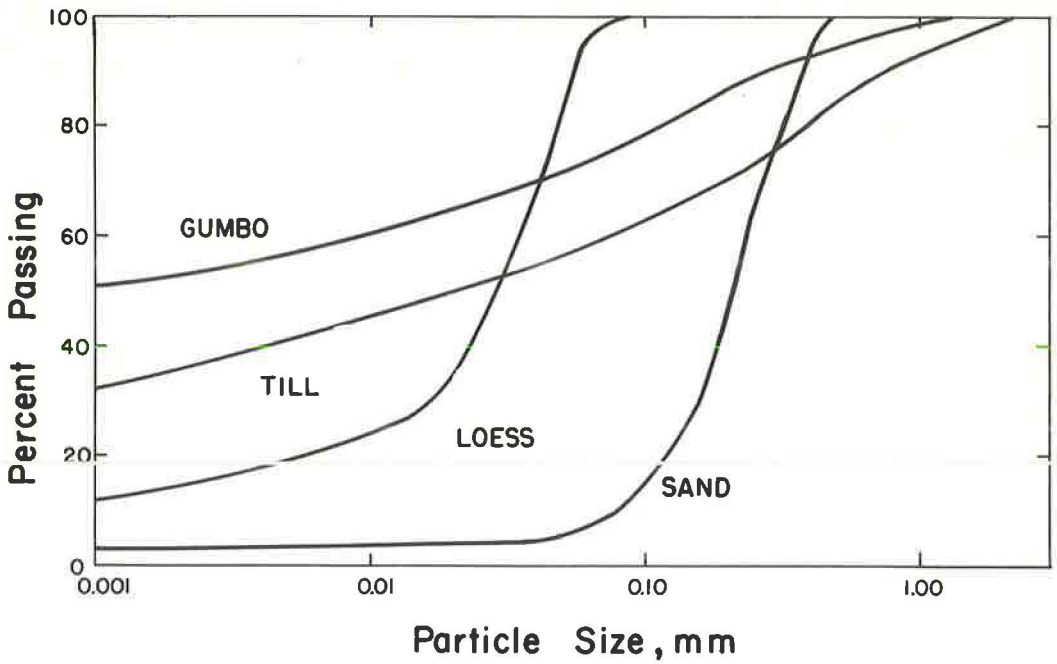

Figure 4. Particle-size accumulation curves of four soils tested for pumping.

Another factor influencing erosion rate is that of protective cover, the most erodible grains will be selectively removed, leaving a lag concentrate or particles with a lower probability of erosion. This is analogous to the desert pavement of wind-swept arid areas. Still another factor is sand-blasting by suspended particles, wherein momentum (mass times velocity) tends to be preserved or transferred to other particles on impact.

TESTS

Four relatively fine-grained soils were selected for test: an aeolian fine sand, a loessial silt, a glacial till loam, and a fossil B-horizon gumbotil clay. Grain size curves are presented in Figure 4; properties are given in Table 1.

The soil samples were molded to either standard or modified Proctor density according to ASTM Designation D 1632-63 (8) for 3- by 3- by 11 ¼-in. flexural test specimens were usually wrapped and allowed to cure at 100 percent humidity 2 days to equilibrate moisture within the sample, release residual stresses, and allow development of thixotropic effect. Most samples swelled during curing and were trimmed back with the aid of a trimming box.

Pumping Action

As the soils pumped, a rigorous erosion action was readily observable through the Plexiglass box front. During the tests, muddy water was squirted about to the extent that splatter shields were added to the apparatus. Typical experimental results are shown in Figure 5. In most instances the slab deflection was proportional to n, the number of repetitions.

Most samples eroded more rapidly under the departure slab, probably because the sudden impact loading of this slab visibly increased fluid ejection velocity. The result was a step analogous to joint faulting in the field (Fig. 6a). Another field condition observed in the model was a tendency to accumulate loose sand back under the slab, which would tend to tilt the slab and accentuate joint faulting if there were no end re-

TABLE 1

PROPERTIES OF SOILS STUDIED

Characteristic	Soil			
	Dune Sand	Friable Loess	Kansan Glacial Till	Gumbotil
Lab No.	S-6-2	20-2	409-C	528-8
Classif.				
AASHO/ASTM	A-3(0)	A-4(8)	A-7-6(14)	A-7-6(20)
BPR	Sand	Silt loam	Clay	Clay
USDA	Sand	Silt	Clay	Clay
County in Iowa	Benton	Harrison	Ringold	Keokuk
Soil series	Carrington	Hamburg	Shelby	Muhaska
Horizon	B	B	B	B
L. L. (%)	-	32	50	65
P. L. (%)	-	27	17	24
P. I.	N. P.	5	33	41
Dom. clay mineral[a]	Mont.	Mont.	Mont.	Mont.
Dom. exch. cation[a]	Ca^{++}	Ca^{++}	Ca^{++}	Ca^{++}

[a]From X-ray diffraction and DTA.

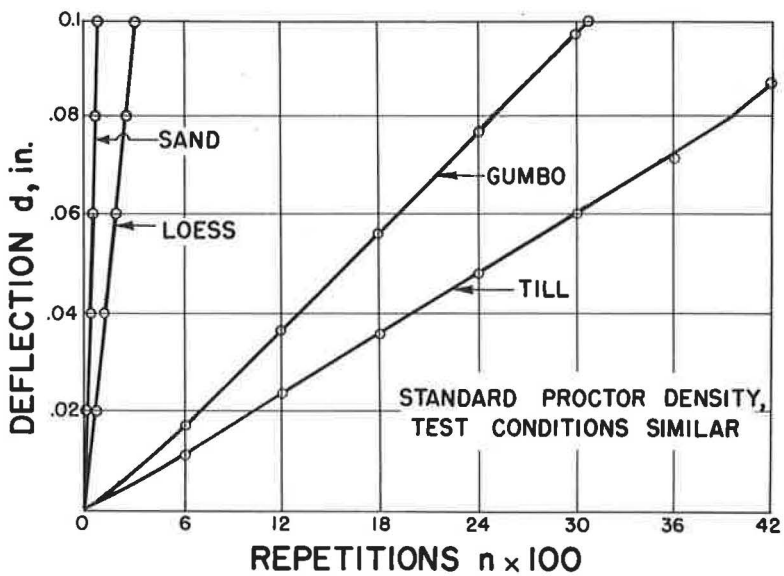

Figure 5. Representative pumping test results.

straints. Clayey samples removed from the machine often showed an interesting pattern of erosion channels between sand-capped mesas (Fig. 6b). Pumping stopped immediately if the water supply was shut off.

Pumping Resistance

Drainage was prevented by the sample box, and the silt and fine sand pumped very rapidly to the arbitrary failure deflection of 0.1 in. (Table 2). The till and gumbotil pumped much more slowly, glacial till being the slowest. Compaction to

TABLE 2

PUMPING TEST RESULTS[a]

Characteristic	Soil											
	Dune Sand			Loess			Glacial Till			Gumbotil		
	Std.	Comp.	Mod. Comp.	Std.	Comp.	Mod. Comp.	Std.	Comp.	Mod. Comp.	Std.	Comp.	Mod. Comp.
Opt. Moist. Cont. (%)	9.5		8.6	15.2		15.0	15.0		12.3	23.2		17.5
Density, pcf	112		118	110		118	116		125	96		109
Direct shear:												
c (psi)	1.6		-	10		-	63		73	40		66
ϕ (deg)	33.9		-	34.0		-	13.8		47.5	8.3		35.0
n for 0.1-in. defl.	47		103	476		500	5,194		5,520	3,049		5,403

[a]All maximum deflections occurred at the joint and on the departure slab.

Figure 6. Tested specimens: (a) top view of gumbo, showing sand-capped mesas, 2,600 repetitions; (b) oblique view of soil-cement showing step, 20,000 repetitions.

modified Proctor density increased pumping resistance, as indicated in Table 2.

Strength Tests

For comparison purposes, direct shear tests were performed on the soil samples, giving c and ϕ values reported in Table 2. The angle of internal friction apparently has little influence on pumping, but cohesion appears closely related to pumping resistance. A graph of n vs c is shown in Figure 7, and gives a linear relationship with a correlation coefficient r = 0.994, a value of 1.0 indicating perfect correlation. Other relationships of n to percent clay, to P. I., to P. I./percent clay, to median grain size, to sorting coefficient, etc., were much less consistent.

Temperature

Tests were made on the silt at different temperatures from 3 to 50 C to find the influence of viscosity and/or changing cohesion. Results are given in Table 3; it will be noted that higher temperatures gave faster pumping.

To determine whether the influence of temperature was one of changing fluid viscosity or changing cohesion, direct shear tests were performed. These gave for the silt:

$$c = 12.5 - \frac{T}{8}$$

where T is degrees centigrade and c is

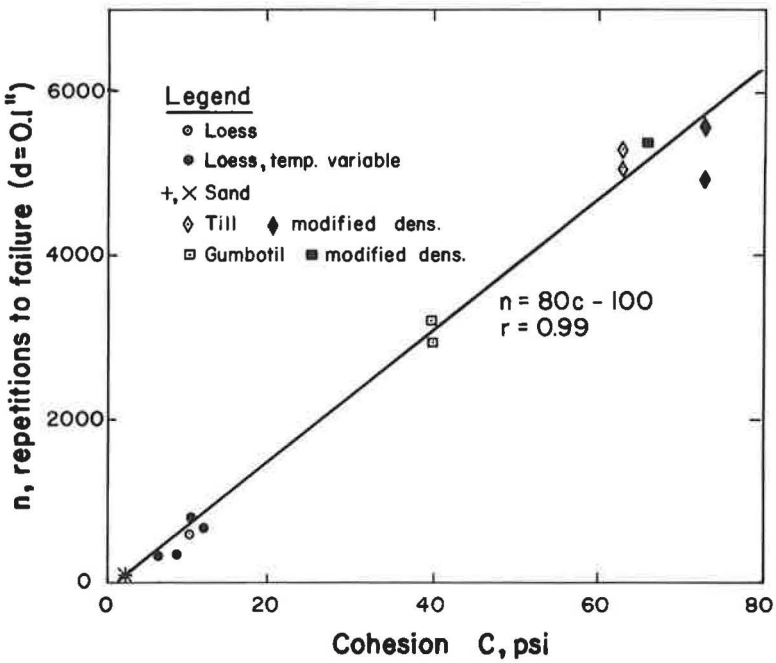

Figure 7. Relation between repetitions to failure and soil cohesion by direct shear test.

TABLE 3

EFFECTS OF TEMPERATURE AND STABILIZERS

Soil	Temperature, °C		Additives	Curing	n for 0.1-in. Defl.
	Soil	Water			
Loess,	3	3	-	-	685
Std.	15.5	15.5	-	-	750
Dens.	21	21	-	-	630
	33	33	-	-	316
	50.5	50.5	-	-	320
Till, mod.	23	22	-	-	5,600
Dens.	5	22	-	-	6,000
Loess	26	26	-	-	335
	26	26	0.2% Arq. 2HT	-	340
	26	26	0.2% Arq. 2HT	2 day air dry	310
75% sand + 25% loess	-	-	6% cement	7 day m.c.	5,500[a]

[a]Data approximate.

cohesion in psi. Points of n vs c corrected for temperature are shown as solid dots in Figure 7 and were included in the correlation analysis. The influence of temperature, therefore, appears to be largely in its effect on soil cohesion.

In one test of glacial till the soil was initially 22 C and the water was 5 C. If viscosity of the water were the controlling factor, retardation of pumping should have been immediate. Instead, no effect was noticed until after about 1,600 repetitions, or 15 min., when the soil apparently cooled sufficiently to retard pumping.

Soaking Effect

The gumbotil clay specimen compacted to modified density was allowed to soak in water 12 hr before testing. There was little or no apparent effect, as is shown in the correlation analysis of Figure 7. Two other tests on the gumbotil at modified density gave higher n's, but were eliminated because of sticking down of the departure slab.

Soil Stabilizers

The results indicate that pumping of fine-grained soils should be controllable by altering their cohesion. To test this premise two stabilizers were tried, a waterproofer and a cementing agent.

An organic cationic water proofer (Armour Co. Arquad 2HT) was selected for the test because it has very little effect on cohesion and when used in optimum amount it imparts water-repellent properties to the soil (15). Results indicated that 0.2 percent cationic waterproofer with and without air curing did not alter pumpability of the loess.

Incorporation of 6 percent cement in a sandy silt base course mix gave n = 5,500, several hundred times more than unstabilized sand. Cohesion of this mix was not measured, but is probably in the range of 20 to 80 psi (16). According to Fig. 7, c should be about 70 psi.)

Further testing was terminated because of lack of research support.

CONCLUSIONS

1. In a model devised to simulate rigid pavement pumping, pumping was observed to be mainly a process of erosion by ejection, which can be stopped by shutting off the water.
2. In an undrained situation or where rainfall exceeds rate of drainage, there is an excellent inverse linear relationship between rate of pumping and soil cohesion as measured by the direct shear test.
3. Modified Proctor compaction reduces pumping by increasing cohesion.
4. Lower soil temperature means slower pumping because of improved cohesion.
5. Cement increases pumping resistance of soils, whereas use of a noncohesive waterproofer does not.
6. Because of the relationships to cohesion, unconfined compressive strength should be an approximate measure of pumping resistance of treated and untreated fine-grained soils.

REFERENCES

1. Yoder, E. J. Principles of Pavement Design. New York, John Wiley and Sons.
2. The AASHO Road Test, Rept. 5, Pavement Research. Highway Research Board Spec. Rept. 61E, 1962.
3. Allen, Harold. Final Report of Project Committee No. 1, Maintenance of Concrete Pavement as Related to the Pumping Action of Slabs. Highway Research Board Proc., Vol. 28, pp. 281-310, 1948.
4. Colley, B. E., and Nowlen, J. W. Performance of Subbases for Concrete Pavements Under Repetitive Loading. Highway Research Board Bull. 202, pp. 32-58, 1958.
5. Havers, J. A., and Yoder, E. J. A Study of Interactions of Selected Combinations of Subgrade and Base Course Subjected to Repeated Loading. Highway Research Board Proc., Vol. 36, pp. 443-478, 1957.

6. Chamberlin, W. P., and Yoder, E. J. Effect of Base Course Gradation on Results of Laboratory Pumping Tests. Highway Research Board Bull. 202, pp. 59-79, 1958.
7. Reign, L. L. Development of an Apparatus and Procedure for Evaluating the Pumping Characteristics of Soil. Iowa State Univ. of Sci. and Tech. Unpubl. M. S. thesis, Ames, Iowa, 1961.
8. 1964 Book of ASTM Standards, Part 11, Amer. Soc. for Testing and Materials, Philadelphia, 1964.
9. Murphy, Glenn. Similitude in Engineering. New York, Ronald Press Co., 1950.
10. Hjulstrom, Filip. Transportation of Detritus by Moving Water. In Trask, Parker D., Recent Marine Sediments, pp. 5-31. Am. Assoc. Pet. Geol. Tulsa, Okla., 1939.
11. Lutz, J. F. The Relation of Soil Erosion to Certain Inherent Soil Properties. Soil Sci. Vol. 40, pp. 439-457, 1935.
12. Leopold, L. B., Wolman, M. G., and Miller, J. P. Fluvial Processes in Geomorphology. San Francisco, W. H. Freeman and Co., 1964.
13. André, J. E., and Anderson, H. W. Variation of Soil Erodibility with Geology, Geographic Zone, Elevation, and Vegetation Type in Northern California Wildlands. Jour. Geophys. Res., Vol. 66, pp. 3351-3358, 1961.
14. Horton, R. E. Erosional Development of Streams and Their Drainage Basins: Hydrophysical Approach to Quantitative Geomorphology. Geol. Soc. Amer. Bull. 54, pp. 275-370, 1945.
15. Hoover, J. M., Davidson, D. T., and Roegiers, J. V. Miniature Triaxial Shear Testing of a Quaternary Ammonium Chloride Stabilized Loess. Iowa Acad. Sci. Proc. 65, pp. 323-331, 1958.
16. Laguros, J. G., and Davidson, D. T. Effect of Chemicals on Soil-Cement Stabilization. Highway Research Record 36, pp. 173-208, 1963.
17. Taylor, Michael A., and Broms, Bergt B. Shear Bond Strength Between Coarse Aggregate and Cement Paste or Mortar. ACI Jour., Proc., Vol. 61, No. 8, pp. 939-957, Aug. 1964.